A New Calibration Method for Strapdown Inertial Navigation Systems

Eun-Hwan Shin and Naser El-Sheimy

Summary

Calibration of inertial instruments is needed because the outputs of instruments contain errors. Current Inertial Navigation Systems (INS) calibration techniques either require specialized calibration facilities or computational methods which make use of the fact that the INS axes should be aligned with local level frame. Furthermore, these calibration techniques are limited in that non-orthogonalities cannot be determined and the misalignment of the Inertial Measurement Unit (IMU) to the local level frame can affect the results. This paper introduces a new calibration method that overcomes these limitations. A mathematical model, which comprises biases, scale factors, and non-orthogonalities, was developed and used in the rigorous least squares adjustment procedure.

The values of gravity and earth rotation rate were used as reference values in the adjustment. The measurement data from eighteen different attitudes are used and the rotation scheme attainable with a two-degree-of-freedom frame is introduced. The test result shows that while biases, scale factors, and non-orthogonalities can be calibrated for the accelerometers, only biases can be calibrated for the gyroscopes. This calibration method can easily be used as a field method.

Zusammenfassung

Instrumentenfehler in inertialen Mess-Systemen machen deren Kalibrierung erforderlich. Heutige INS Kalibrierungstechniken benötigen jedoch entweder spezielle Kalibrierungseinrichtungen oder Computermethoden, die die Ausrichtung der Achsen bezüglich eines lokalen Systems ausnutzen. Darüberhinaus sind diese Kalibrierungsmethoden durch Nicht-Rechtwinkligkeiten und falsche Ausrichtungen der IMU's bezüglich des lokalen Bezugssystems limitiert, die die Ergebnisse weiter beeinflussen können. Dieser Artikel führt eine neue Kalibrierungsmethode ein, die diese Restriktionen überwindet. Ein mathematisches Modell wurde entwickelt, das die Nicht-Rechtwinkligkeiten, den Maßstab und systematische Fehler mit der strengen kleinsten Quadrate Methode verbindet.

Schwerewerte und die Erdrotationsgeschwindigkeit wurden als Referenzwerte in die Ausgleichung eingeführt. Messwerte von achtzehn verschiedenen Positionen und das Rotationsschema, welches für einen Kardanrahmen mit zwei Freiheitsgraden eingesetzt werden kann, wurden verwendet. Die Ergebnisse zeigen deutlich, dass systematische Fehler, der Maßstabsfaktor und Nicht-Rechtwinkligkeiten für die Beschleuningungsmesser kalibriert werden können, während für die Kreisel nur systematische Fehler berechnet werden können. Diese Kalibrierungsmethode kann auch unter Nichtlaborbedingungen verwendet werden.

1 Introduction

Inertial Navigation Systems (INS) made their appearance in commercial aviation in the late sixties and have been extensively used in intercontinental navigation and in flight control systems. Their distinctive characteristic is the capability for autonomous navigation in any environment. They operate without reference to external signal and therefore are not affected by atmospheric condition or line of sight obstruction and usable in underwater or underground operation. This feature attracted major military research funding and the vigorous development of inertial components and systems over the last thirty years can be mainly attributed to this interest (Krakiwsky 1990). At present, there is no sign that this development is slowing down, for more details on the future of inertial navigation systems see Schwarz and El-Sheimy (1999).

The *principle of inertial navigation* is based on Newton's first and second law of motion. Measuring vehicle acceleration in an inertial frame of reference, integrating it with respect to time and transforming it to the navigation frame can obtain velocity, attitude and position differences in the navigation frame. In this mode of operation, an INS can be considered as a highly sophisticated dead-reckoning system. Sensors used to implement such a system are accelerometers for the measurement of specific force and gyroscopes for the implementation of an inertial frame of reference. Since specific force measurements contain the effect of the gravity field of the earth, a gravity model is needed to extract vehicle acceleration from the measurements. Because they employ three-translational and three-rotational sensors, inertial measuring units can be used as positioning as well as attitude sensing devices.

The performance of INS can be described in terms of its two major groups of sensors, i. e. gyroscopes and accelerometers. Gyroscopes are angular rate sensors. They output either angular rate or attitude, depending on whether they are of the rate sensing or rate integrating type. Measurements of the angular rate can be modeled by the following observation equation (Schwarz and Wei 2000):

$$l_\omega = \omega + d + S\omega + N\omega + \varepsilon_\omega \qquad (1)$$

where l_ω is the measurement, ω is the angular velocity, d is the gyroscope instrument bias, S is a matrix representing the gyroscope scale factor, N is a matrix representing non-orthogonality of the gyroscope triad, ε_ω is a vector representing the gyroscope sensor noise.

Gyro performance is expressed by its scale factor stability and bias. Scale factor stability is the capability of the gyro to accurately sense angular velocity at different angular rates. Deviations from the theoretical scale are due to system imperfections. They cause small variations in the scale, which multiply into the rotation rate. Gyro bias characterizes the capability of the gyro to reference all rate measurements to the nominal zero point. It therefore appears as an additive term to the gyro output rate. Figure 1 shows the performance of current and future gyro technologies.

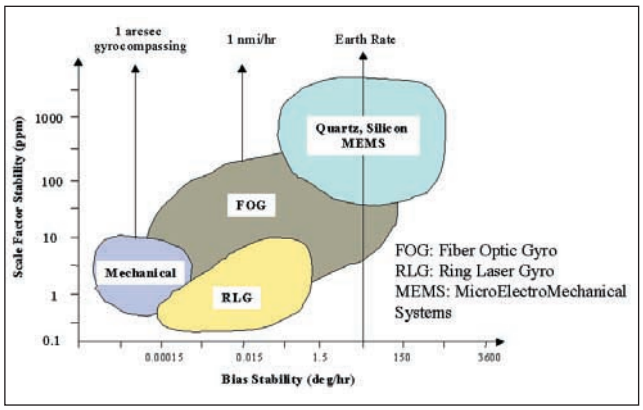

Fig. 1: Performance of Current and Future Gyro Technology

Accelerometers are specific force sensors whose output is specific force or, in case of integrating accelerometers, velocity. They provide the sensor output that is essential for positioning. Figure 2 shows the performance of current and future accelerometer technologies, for more details see (Greenspan 1995).

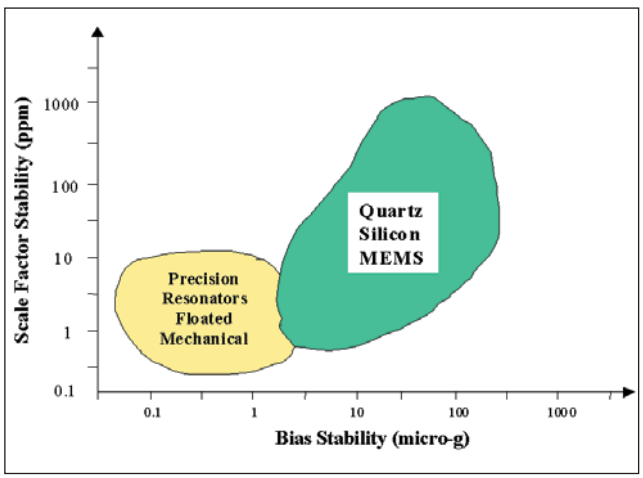

Fig. 2: Performance of Accelerometer Technology

Performance factors describing accelerometer accuracy are similar to those characterizing gyro accuracy: Scale factor stability and asymmetry, bias uncertainty, and random and quantizer noise. Measurements of the specific force can be modeled by the following observation equation (Schwarz and Wei 2000):

$$l_g = f + b + (S_1 + S_2 f)f + Nf + \gamma + \delta g + \varepsilon_f \qquad (2)$$

where l_g is the measurement, f is the specific force (observable), S_1 is a matrix representing the linear scale factor errors, S_2 is a matrix representing the non-linear scale factor errors, N is a matrix representing the non-orthogonality of the axes, γ is the vector of normal gravity, δg is the anomalous gravity vector, and ε_f is noise.

2 INS Calibration Methods

Calibration of inertial instruments is needed because the outputs of instruments contain errors. Chatfield (1997) defined calibration as the process of comparing instrument outputs with known reference information and determining coefficients that force the output to agree with the reference information over a range of output values. Calibration parameters to be determined can change according to the specific technology in an inertial measurement unit (IMU). To accurately determine all parameters special calibration devices are needed such as three-axial turn tables or special techniques which can be classified as follows:

Local Level Frame (LLF) Calibration: In this calibration method, the INS systems involve mounting the unit on a multi-axes turntable whose axes are oriented precisely with respect to the LLF. The unit is then be rotated through series of accurately known angles and positioned in different orientation with respect to the LLF. Dominant sensor errors may be then determined from static measurements of acceleration and angular rate taken in each orientation of the unit. For more details, see Salychev (1998). This calibration method has two main drawbacks:

a) The small magnitude of the Earth's rotation usually leads to difficulties in estimating the gyro biases
b) It requires the alignment of the INS axes with respect to the LLF. Any orientation errors will influence the calibration accuracy

Six-position Static Acceleration Tests: This category is special case of the first type in which the inertial system is mounted on a level table with each sensitive axis pointing alternately up and down (six positions). Therefore, it is possible to extract estimates of the accelerometer bias and scale factor by summing and differencing combinations of the inertial system measurements. For

example, the calibration procedure for a z-axis accelerometer is shown in Figure 3.

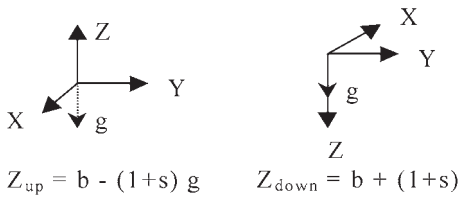

Fig. 3: Six-position Static Tests

The bias and scale factor of the Z-accelerometer can be calculated from these measurements as:

$$b = (Z_{up} + Z_{down}) / 2,\ s = (Z_{down} - Z_{up} - 2g) / 2g$$

where b, s and g represent bias, scale factor and gravity, respectively.

The limitations of this method are that the non-orthogonality cannot be determined and that the misalignment of the IMU sensitive axes under investigation with respect to the vertical direction can affect the result even though it is very small (Rogers 2000).

Angle Rate Tests: Using a precision rate table, the IMU may be rotated through very accurately known angles. By comparing these known rotations with estimates of the angles turned through by the systems, derived by integrating the rate outputs provided by the gyros, it is possible to derive estimates of the various errors in the gyros measurements. For instance, if the table is rotated clockwise and counter-clockwise through the same angle, estimates of the gyro biases and scale factors errors can be estimated. For more details, see Titterton and Weston (1997).

This paper introduces a new calibration procedure that can be used in cases where no elaborate lab instrumentation is available. With some modifications, they could also be used as field procedures. The new calibration models can be used for the determination of bias, scale factor, and non-orthogonality for a triad of accelerometers and a triad of gyroscopes without aligning the IMU precisely to the local-level frame or requiring the knowledge of the INS axes. These parameters are common to all types of strapdown IMUs and are the most important ones. Of these parameters, the bias can change from switch-on to switch-on (Titterton and Weston 1997). Because the models developed basically do not dependent on the attitude of the IMU to be calibrated, it will be possible to calibrate an IMU in the field right before starting a mission. In the calibration procedure, the values of gravity and the earth's rotation rate will be used as reference values for accelerometers and gyroscopes, respectively.

In section 3 the calibration models for this system will be derived. Considerations about adjustment computations will be discussed in section 4. Section 5 deals with results of numerical calculations and conclusions will be given in section 6.

3 Calibration Models

3.1 Consideration of non-orthogonality

All vectors in R^3 space can be expressed as linear combinations of the following three-orthonormal vectors that correspond to the three orthogonal axes of accelerometers or gyroscopes of an IMU:

$$x: (1, 0, 0),\ y: (0, 1, 0),\ z: (0, 0, 1). \tag{3}$$

The values sensed by each of these axes can be expressed using the inner products of the measurement vector and the orthonormal vectors, for instance as shown for the gravity vector g: (g_x, g_y, g_z):

$$\begin{aligned} g_x &= \prec g, x \succ = g\cos\alpha, \\ g_y &= \prec g, y \succ = g\cos\beta, \\ g_z &= \prec g, z \succ = g\cos\gamma \end{aligned} \tag{4}$$

where, $\prec\cdot,\cdot\succ$ denotes the inner product and α, β, γ are angles generated by the gravity vector and x, y, z axis, respectively.

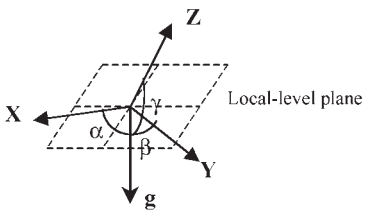

Fig. 4: Misalignment to the local-level frame

The following characteristic holds regardless of the misalignment to a local-level frame and plays a fundamental role in this derivation:

$$g_x^2 + g_y^2 + g_z^2 = |g|^2 \left(\cos^2\alpha + \cos^2\beta + \cos^2\gamma\right) = |g|^2 . \tag{5}$$

In reality, the three axes of accelerometers or gyroscopes of an IMU may not be perfectly orthogonal to each other. As shown in Figure 5, when the y-axis is rotated by the angle θ_{yz}, this rotated axis can be represented as following unit vector:

$$y_1 : (-\sin\theta_{yz}, \cos\theta_{yz}, 0) = R_z y \tag{6}$$

where,

$$R_z = \begin{pmatrix} \cos\theta_{yz} & -\sin\theta_{yz} & 0 \\ \sin\theta_{yz} & \cos\theta_{yz} & 0 \\ 0 & 0 & 1 \end{pmatrix}.$$

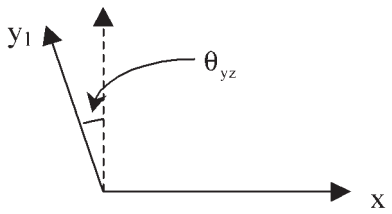

Fig. 5: Non-orthogonality between x and y

In R^3 space, the non-orthogonality of the z-axis, for example, can be expressed by successive two rotations, i. e. a rotation with respect to x-axis with the angle θ_{zx} and a rotation about the y-axis with the angle θ_{yz} (see Figure 6). This non-orthogonal z-axis can again be represented using the following unit vector

$$z_1 : (\sin\theta_{zy}, -\sin\theta_{zx}\cos\theta_{zy}, \cos\theta_{zx}\cos\theta_{zy}) = R_x R_y z \qquad (7)$$

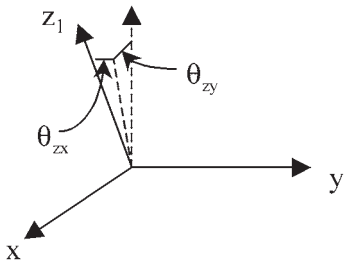

Fig. 6: Non-orthogonality of z-axis to xy plane

where R_x and R_y are rotation matrices for a vector with respect to x-axis and y-axis, respectively, and defined by

$$R_x = \begin{pmatrix} 1 & 0 & 0 \\ 0 & \cos\theta_{zx} & -\sin\theta_{zx} \\ 0 & \sin\theta_{zx} & \cos\theta_{zx} \end{pmatrix}; \quad R_y = \begin{pmatrix} \cos\theta_{zy} & 0 & \sin\theta_{zy} \\ 0 & 1 & 0 \\ -\sin\theta_{zy} & 0 & \cos\theta_{zy} \end{pmatrix}.$$

Hence, considering non-orthogonality of θ_{yz}, θ_{zx}, and θ_{zy}, all vectors in R^3 space can be expressed as linear combinations of the following three vectors that correspond to three non-orthogonal axes of accelerometers or gyroscopes of an IMU:

$$\begin{aligned} &x_1 : (1,0,0), \\ &y_1 : (-\sin\theta_{yz}, \cos\theta_{yz}, 0), \\ &z_1 : (\sin\theta_{zy}, -\sin\theta_{zx}\cos\theta_{zy}, \cos\theta_{zx}\cos\theta_{zy}). \end{aligned} \qquad (8)$$

The values to be sensed by each of these non-orthogonal axes can be expressed using again the inner product, for instance for gravity vector g: (g_x, g_y, g_z),

$$\begin{aligned} &g_{x1} = < g, x_1 > = g_x, \\ &g_{y1} = < g, y_1 > = -g_x \sin\theta_{gyz} + g_y \cos\theta_{gyz}, \\ &g_{z1} = < g, z_1 > = g_x \sin\theta_{gzy} - g_y \sin\theta_{gzx}\cos\theta_{gzy} + g_z \cos\theta_{gzx}\cos\theta_{gzy}. \end{aligned} \qquad (9)$$

3.2 A New IMU Calibration Method

The new calibration method makes use of the fact that regardless the direction of the INS axes, the total values sensed by the accelerometers and the gyroscopes should be equal to the gravity and earth rotation values, respectively. Taking biases, scale factors, and misalignments into account, the values to be measured as a result of the gravity vector g can be written as:

$$\begin{aligned} &l_{gx} = b_{gx} + (1+s_{gx})g_x, \\ &l_{gy} = b_{gy} + (1+s_{gy})(-g_x \sin\theta_{gyz} + g_y \cos\theta_{gyz}), \\ &l_{gz} = b_{gz} + (1+s_{gz})(g_x \sin\theta_{gzy} - g_y \sin\theta_{gzx}\cos\theta_{gzy} + g_z \cos\theta_{gzx}\cos\theta_{gzy}) \end{aligned} \qquad (10)$$

where, b and s represent bias and scale factor, respectively.

Rearranging equation (10) we can obtain the following values for the gravity vector components:

$$\begin{aligned} g_x &= \frac{l_{gx} - b_{gx}}{1+s_{gx}} \\ g_y &= \tan\theta_{gyz}\left(\frac{l_{gx} - b_{gx}}{1+s_{gx}}\right) + \left(\frac{1}{\cos\theta_{gyz}}\right)\left(\frac{l_{gy} - b_{gy}}{1+s_{gy}}\right) \\ g_z &= \left(\tan\theta_{gzx}\tan\theta_{gyz} - \frac{\tan\theta_{gzy}}{\cos\theta_{gzx}}\right)\left(\frac{l_{gx} - b_{gx}}{1+s_{gx}}\right) \\ &\quad + \left(\frac{\tan\theta_{gzx}}{\cos\theta_{gyz}}\right)\left(\frac{l_{gy} - b_{gy}}{1+s_{gy}}\right) \\ &\quad + \left(\frac{1}{\cos\theta_{gzx}\cos\theta_{gzy}}\right)\left(\frac{l_{gz} - b_{gz}}{1+s_{gz}}\right). \end{aligned} \qquad (11a)$$

Following the same procedure, equations for gyroscopes will be

$$\begin{aligned} \omega_x &= \frac{l_{\omega x} - b_{\omega x}}{1+s_{\omega x}} \\ \omega_y &= \tan\theta_{\omega yz}\left(\frac{l_{\omega x} - b_{\omega x}}{1+s_{\omega x}}\right) + \left(\frac{1}{\cos\theta_{\omega yz}}\right)\left(\frac{l_{\omega y} - b_{\omega y}}{1+s_{\omega y}}\right) \\ \omega_z &= \left(\tan\theta_{\omega zx}\tan\theta_{\omega yz} - \frac{\tan\theta_{\omega zy}}{\cos\theta_{\omega zx}}\right)\left(\frac{l_{\omega x} - b_{\omega x}}{1+s_{\omega x}}\right) \\ &\quad + \left(\frac{\tan\theta_{\omega zx}}{\cos\theta_{\omega yz}}\right)\left(\frac{l_{\omega y} - b_{\omega y}}{1+s_{\omega y}}\right) \\ &\quad + \left(\frac{1}{\cos\theta_{\omega zx}\cos\theta_{\omega zy}}\right)\left(\frac{l_{\omega z} - b_{\omega z}}{1+s_{\omega z}}\right). \end{aligned} \qquad (11b)$$

Using equations (11) we can define a general mathematical model for the calibration of a triad of accelerometers by

$$f_g = g_x^2 + g_y^2 + g_z^2 - |g|^2 = 0 \ , \tag{12a}$$

and for a triad of gyroscopes by

$$f_\omega = \omega_x^2 + \omega_y^2 + \omega_z^2 - |\omega|^2 = 0 \ . \tag{12b}$$

By substituting equation (11) into (12), we can get

$$\begin{aligned} f_g = &\left[\frac{l_{gx} - b_{gx}}{1+s_{gx}}\right]^2 + \left[\tan\theta_{gyz}\left(\frac{l_{gx} - b_{gx}}{1+s_{gx}}\right) + \left(\frac{1}{\cos\theta_{gyz}}\right)\left(\frac{l_{gy} - b_{gy}}{1+s_{gy}}\right)\right]^2 \\ &+ \left[\left(\tan\theta_{gzx}\tan\theta_{gyz} - \frac{\tan\theta_{gzy}}{\cos\theta_{gzx}}\right)\left(\frac{l_{gx} - b_{gx}}{1+s_{gx}}\right) + \left(\frac{\tan\theta_{gzx}}{\cos\theta_{gyz}}\right)\left(\frac{l_{gy} - b_{gy}}{1+s_{gy}}\right)\right. \\ &\left. + \left(\frac{1}{\cos\theta_{gzx}\cos\theta_{gzy}}\right)\left(\frac{l_{gz} - b_{gz}}{1+s_{gz}}\right)\right]^2 - |g|^2 = 0, \end{aligned} \tag{13a}$$

$$\begin{aligned} f_\omega = &\left[\frac{l_{\omega x} - b_{\omega x}}{1+s_{\omega x}}\right]^2 + \left[\tan\theta_{\omega yz}\left(\frac{l_{\omega x} - b_{\omega x}}{1+s_{\omega x}}\right) + \left(\frac{1}{\cos\theta_{\omega yz}}\right)\left(\frac{l_{\omega y} - b_{\omega y}}{1+s_{\omega y}}\right)\right]^2 \\ &+ \left[\left(\tan\theta_{\omega zx}\tan\theta_{\omega yz} - \frac{\tan\theta_{\omega zy}}{\cos\theta_{\omega zx}}\right)\left(\frac{l_{\omega x} - b_{\omega x}}{1+s_{\omega x}}\right) + \left(\frac{\tan\theta_{\omega zx}}{\cos\theta_{\omega yz}}\right)\left(\frac{l_{\omega y} - b_{\omega y}}{1+s_{\omega y}}\right)\right. \\ &\left. + \left(\frac{1}{\cos\theta_{\omega zx}\cos\theta_{\omega zy}}\right)\left(\frac{l_{\omega z} - b_{\omega z}}{1+s_{\omega z}}\right)\right]^2 - |\omega|^2 = 0. \end{aligned} \tag{13b}$$

To check for any time varying factors in the accelerometer calibration, the following two models can be used:

$$\begin{aligned} l_{gx} &= b_{gx} + d_{gx}t + g_x; \\ l_{gy} &= b_{gy} + d_{gy}t + g_y; \\ l_{gz} &= b_{gz} + d_{gz}t + g_z \end{aligned} \tag{14}$$

and

$$\begin{aligned} l_{gx} &= b_{gx} + d_{gx}t + dd_{gx}t^2 + g_x \\ l_{gy} &= b_{gy} + d_{gy}t + dd_{gy}t^2 + g_y \\ l_{gz} &= b_{gz} + d_{gz}t + dd_{gz}t^2 + g_z \end{aligned} \tag{15}$$

where d_{gx}, d_{gy}, d_{gz} are the linear drift parameters, and dd_{gx}, dd_{gy}, dd_{gz} are the second-order drift parameters.

For the gyroscope calibration various combinations of parameters were tested. At first, by setting $s_{\omega x} = s_{\omega y} = s_{\omega z} = \theta_{\omega yz} = \theta_{\omega zx} = \theta_{\omega zy} = 0$ in equation (13b), the bias-only model can be derived:

$$\omega_x = l_{\omega x} - b_{\omega x}; \quad \omega_y = l_{\omega y} - b_{\omega y}; \quad \omega_z = l_{\omega z} - b_{\omega z} \ . \tag{16}$$

Secondly, by setting $\theta_{\omega yz} = \theta_{\omega zx} = \theta_{\omega zy} = 0$ in equation (13b), the bias and scale factor model can be derived:

$$\omega_x = \frac{l_{\omega x} - b_{\omega x}}{1+s_{\omega x}}; \quad \omega_y = \frac{l_{\omega y} - b_{\omega y}}{1+s_{\omega y}}; \quad \omega_z = \frac{l_{\omega z} - b_{\omega z}}{1+s_{\omega z}} \ . \tag{17}$$

Thirdly, the bias and non-orthogonality model can be derived by setting $s_{\omega x} = s_{\omega y} = s_{\omega z} = 0$ in equation (13b):

$$\begin{aligned} \omega_x &= l_{\omega x} - b_{\omega x} \\ \omega_y &= \tan\theta_{\omega yz}(l_{\omega x} - b_{\omega x}) + (l_{\omega y} - b_{\omega y})/\cos\theta_{\omega yz} \\ \omega_z &= \left(\tan\theta_{\omega zx}\tan\theta_{\omega yz} - \frac{\tan\theta_{\omega zy}}{\cos\theta_{\omega zx}}\right)(l_{\omega x} - b_{\omega x}) \\ &+ \left(\frac{\tan\theta_{\omega zx}}{\cos\theta_{\omega yz}}\right)(l_{\omega y} - b_{\omega y}) + \frac{(l_{\omega z} - b_{\omega z})}{\cos\theta_{\omega zx}\cos\theta_{\omega zy}} \end{aligned} \tag{18}$$

Finally the bias and drift model was tested.

$$\begin{aligned} l_{\omega x} &= b_{\omega x} + d_{\omega x}t + \omega_x; \\ l_{\omega y} &= b_{\omega y} + d_{\omega y}t + \omega_y; \\ l_{\omega z} &= b_{\omega z} + d_{\omega z}t + \omega_z \end{aligned} \ . \tag{19}$$

The estimated biases and their standard deviations from the simple model described by equation (16) were used as initial information for other gyroscope calibration model adjustments.

4 Adjustment Computation

The implicit mathematical models, equations (13a) and (13b), were implemented in adjustment procedures using the combined case with weighed parameters Least Squares, for detail refer to Krakiwsky (1990):

$$A\hat{\delta} + B\hat{r} + w = 0 \ ; \ \hat{x} = x + \hat{\delta} \ ; \ \hat{l} = l + \hat{r} \tag{20}$$

where, for the measurements of a triad of accelerometers i. e. equation (13a), the design matrices A and B are given by

$$A = \begin{pmatrix} \cdots & \cdots & \cdots & \cdots & \cdots & \cdots & \cdots & \cdots & \cdots \\ \frac{\partial f_g}{\partial b_{gx}} & \frac{\partial f_g}{\partial b_{gy}} & \frac{\partial f_g}{\partial b_{gz}} & \frac{\partial f_g}{\partial s_{gx}} & \frac{\partial f_g}{\partial s_{gx}} & \frac{\partial f_g}{\partial s_{gx}} & \frac{\partial f_g}{\partial \theta_{gyz}} & \frac{\partial f_g}{\partial \theta_{gzx}} & \frac{\partial f_g}{\partial \theta_{gzy}} \\ \cdots & \cdots & \cdots & \cdots & \cdots & \cdots & \cdots & \cdots & \cdots \end{pmatrix}$$

$$B = \begin{pmatrix} \cdots & \cdots & \cdots & & & & & & \\ & & & \frac{\partial f_g}{\partial l_{gx}} & \frac{\partial f_g}{\partial l_{gy}} & \frac{\partial f_g}{\partial l_{gz}} & & & \\ & & & & & & \cdots & \cdots & \cdots \end{pmatrix},$$

where

$\hat{\delta}$ is the correction vector

$$\delta = \left(\delta b_{gx} \quad \delta b_{gy} \quad \delta b_{gz} \quad \delta s_{gx} \quad \delta s_{gy} \quad \delta s_{gz} \quad \delta\theta_{gyz} \quad \delta\theta_{gzx} \quad \delta\theta_{gzy}\right)^T$$

$\hat{r}$ is the vector of residuals

$$\hat{r} = \left(\cdots \quad \cdots \quad \cdots \quad r_{gx} \quad r_{gy} \quad r_{gz} \quad \cdots \quad \cdots \quad \cdots\right)^T,$$

w is the misclosure vector

$$w = \left(\cdots \quad f_g(x,l) \quad \cdots\right)^T,$$

l is the vector of observations.

The elements of the design matrices A and B are given in Appendix (1). The equations for the measurements of a triad of gyroscopes have the same structure.

The solution of this system of equations is given by

$$\hat{\delta} = -N^{-1}u = -\left[A^T\left(BC_lB^T\right)^{-1}A + C_x^{-1}\right]^{-1}A^T\left(BC_lB^T\right)^{-1}w \tag{21}$$

$$C_{\hat{x}} = N^{-1} = \left[A^T\left(BC_lB^T\right)^{-1}A + C_x^{-1}\right]^{-1} \tag{22}$$

where N is the coefficient matrix of the normal equations.

If the measurements are uncorrelated, C_l will be diagonal and $\left(BC_lB^T\right)^{-1}$ will be diagonal as well. Then, the diagonal element corresponding to the i-th measurement take the form:

$$M_{ii}^{-1} = \left(BC_lB^T\right)^{-1}_{ii} = \left[\sigma^2_{lgx}\left(\frac{\partial f_g}{\partial l_{gx}}\right)^2 + \sigma^2_{lgy}\left(\frac{\partial f_g}{\partial l_{gy}}\right)^2 + \sigma^2_{lgz}\left(\frac{\partial f_g}{\partial l_{gz}}\right)^2\right]^{-1}_i . \tag{23}$$

Hence, the normal matrix will be symmetric and we can directly compose the coefficient matrix of the normal equation without generating intermediate matrices, i. e. A and B, as follows:

$$N_{ij} = \sum_k A_{ki}M_{kk}^{-1}A_{kj} + \left(C_x^{-1}\right)_{ij},$$
$$i = 1,2,\cdots,9. \quad j = i, i+1,\cdots,9. \tag{24}$$
$$u_i = \sum_k A_{ki}M_{ii}^{-1}w_i, \quad i = 1,2,\cdots,9.$$

The equations for the adjustment computation of gyroscope measurements have the same structure. Using these equations and the widely used numerical algorithm such as Cholesky's decomposition, we can significantly reduce the amount of memory required for storing the matrices.

Although this method does not require the IMU axes to be aligned to the local-level frame, to avoid singularity in the calculation of the inverse of the normal matrix, at least nine different attitudes should be measured. As shown in Figure 7, possible attitudes would be each face down, each side down and each corner down, which make for six, twelve, and eight different attitude measurements, respectively. Because the non-orthogonality is not changing in time, the number of parameters can be changed to the need, however. We can use an existing value for non-orthogonality from a previous calibration. In that case the number of the parameters will be reduced to six. Therefore, we only need measurements from six different attitudes in the field.

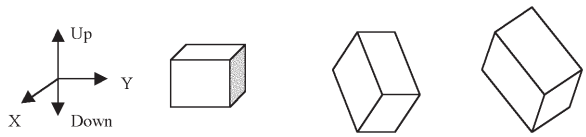

Fig. 7: IMU measurement attitudes

For a triad of accelerometers, the attitudes of each face down should be enough for the determination of the bias and scale factor. Because the attitudes of each side down and each corner down correspond to the relationship between the two axes and three axes in an IMU, they are enough for the determination of the non-orthogonalities.

For a triad of gyroscopes, the number of axes that have values significantly larger than zero can change according to the latitude and the azimuth of an IMU. In mid-latitude areas, when one of the three axes points to east or west, the number can be two for the attitudes of each face down, one for those of each side down, and two for those of each corner down. Figure 8 shows an example of

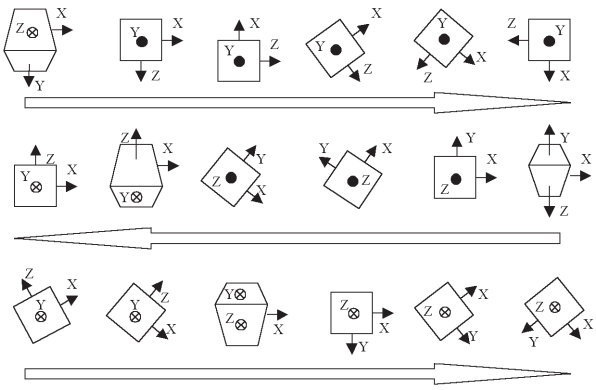

Fig. 8: An example of IMU rotation scheme

rotation schemes for eighteen different measurements, which can be implemented using two-degree-of-freedom cardinal frames.

5 Experiments and Analysis of Results

To test the newly developed method, a series of tests were conducted on two types of IMUs, Litton LTN-90-100 and Honeywell HG1700. The LTN-90-100 is RLG-based navigation-grade system rated at 0.01 deg/hr while the HG1700 is RLG-based tactical grade system rated at 1–3 deg/hr. Table (1) lists the manufacturer's specification of both systems. For all different attitudes setup, averaged values of five-minute measurements were used as input data to the adjustment. To check the long-term variations, six calibrations were done from August 08 to February 12, 2001 for the LTN-90-100 system.

		LTN-90-100	HG1700
GYRO	Input Range		± 1,000 deg/sec
	Scale Factor	5 ppm	100 ppm
	Bias	0.01 deg/hr	1.0 ~ 10 deg/hr
	Non-orthogonality	2 arc sec	
	Random Walk	0.002 deg/√hr	0.125~0.3 deg/√hr
ACCEL	Range		± 50 g
	Linearity		500 ppm
	Scale Factor	50 ppm	300 ppm
	Bias	50 mGal	1.0 mg
	Non-orthogonality	5 arc sec	
	Random Walk	5 mGal	

Table 1: IMU specifications

5.1 Accelerometer Adjustments

Table 2 shows the adjustment results for the six calibrations of LTN-90-100 using the same initial values. The biggest variation (about 25 mGal) was found in y-bias from switch-on to switch-on. Scale factors and non-orthogonalities are quite consistent for all data sets and the standard deviations are small compared to the parameters. All the parameters, except z-bias, are quite close to the specifications given by the manufacturer. Table 3 shows the accelerometer calibration results using previously adjusted results as initial values.

By comparing the results in Table 2 and Table 3, we can see that for most data sets the variance factors in Table 3 are bigger than those in Table 2. Hence, using previously adjusted parameters and their covariance information as inputs to the next adjustment does not guarantee better adjustment results because of the randomness in the changes of biases that are biggest factors.

Considering the biases as constants by using the results given in Table 2, i. e. removing biases from parameters, the first and second-order time dependent models were tested. Although the adjustments converged rapidly, the standard deviations were almost at the same level as the parameters themselves.

The same method was applied to the Honeywell HG1700 which has relatively high performance considering its low cost (about $12,000US). Tables 4 and 5 show the calibration result of this system. Although the biases are much bigger than those of LTN-90-100, the adjustment showed rapid convergence and the standard deviations of the parameters are small enough. Therefore, the newly developed calibration method proved to work as well for low cost IMU systems.

		Bias (mGal)			Scale factor (ppm)			Non-orthogonality (arc sec)			$\hat{\sigma}_0^2$
		X	Y	Z	X	Y	Z	θ_{gyz}	θ_{gzx}	θ_{gzy}	
AUG 08	Value	41.0	-3.1	121.0	-97.0	-71.0	-82.9	-5.9	-3.0	4.5	0.0355
	SD	0.6	0.5	0.6	0.8	0.7	0.7	0.3	0.3	0.3	
AUG 09	Value	45.8	-8.3	119.9	-105.3	-79.6	-92.9	-5.4	-2.7	5.1	0.0452
	SD	0.6	0.6	0.6	0.8	0.7	0.7	0.3	0.3	0.3	
NOV 12	Value	31.4	16.8	115.3	-109.9	-71.6	-93.0	-4.5	-5.3	3.9	0.0398
	SD	0.6	0.6	0.6	0.7	0.7	0.7	0.3	0.3	0.3	
NOV 13	Value	38.5	6.9	115.1	-89.3	-55.1	-66.9	-4.6	-5.0	4.5	0.0132
	SD	0.6	0.6	0.6	0.7	0.7	0.7	0.3	0.3	0.3	
DEC 14	Value	50.3	-9.7	112.4	-110.1	-70.8	-85.6	-4.5	-3.4	4.2	0.0147
	SD	0.6	0.6	0.6	0.7	0.7	0.7	0.3	0.3	0.3	
FEB 12	Value	47.9	-3.7	112.8	-105.2	-63.0	-71.4	-4.6	-5.9	3.7	0.0129
	SD	0.6	0.6	0.5	0.7	0.8	0.7	0.3	0.3	0.3	

Table 2: LTN-90-100 accelerometer calibration results (300 iterations) using the same initial values

		Bias (mGal)			Scale factor (ppm)			Non-orthogonality (arc sec)			$\hat{\sigma}_0^2$
		X	Y	Z	X	Y	Z	θ_{gyz}	θ_{gzx}	θ_{gzy}	
AUG 08	Value	41.0	-3.1	121.0	-97.0	-71.0	-82.9	-5.9	-3.0	4.5	0.0355
	SD	0.6	0.5	0.6	0.8	0.7	0.7	0.3	0.3	0.3	
AUG 09	Value	43.7	-5.6	120.5	-101.7	-75.1	-87.9	-5.7	-2.9	4.8	0.0862
	SD	0.4	0.4	0.4	0.6	0.5	0.5	0.2	0.2	0.2	
NOV 12	Value	39.2	1.4	118.7	-104.6	-74.2	-89.5	-5.1	-3.8	4.6	0.2420
	SD	0.3	0.3	0.3	0.4	0.4	0.4	0.2	0.2	0.2	
NOV 13	Value	39.0	2.7	117.8	-100.3	-69.8	-83.9	-5.0	-4.1	4.6	0.3764
	SD	0.3	0.3	0.3	0.4	0.4	0.4	0.2	0.1	0.1	
DEC 14	Value	41.3	0.3	116.7	-102.4	-70.0	-84.2	-4.9	-4.0	4.5	0.1585
	SD	0.3	0.3	0.2	0.3	0.3	0.3	0.1	0.1	0.1	
FEB 12	Value	42.5	-0.2	116.1	-102.9	-69.2	-81.7	-4.8	-4.3	4.4	0.1128
	SD	0.2	0.2	0.2	0.3	0.3	0.3	0.1	0.1	0.1	

Table 3: LTN 90-100 accelerometer calibration results (300 iterations) using previously adjusted results as initial values

Attitude		Accelerometer		Gyroscope	
		Mean (m/s^2)	STD (mGal)	Mean (deg/h)	STD (deg/h)
X	Up	-9.649	30.685	14.616	0.6550
	Down	9.643	29.858	-7.957	0.7253
Y	Down	9.795	32.634	-12.628	0.7379
Z	Up	-9.803	22.949	10.535	2.2369
	Down	9.812	24.725	-12.584	2.4336

Table 4: HG1700 observations

Parameter	Nov. 15	
	Value	STD
x-bias (mGal)	317.1287	0.7577
y-bias (mGal)	-95.8025	1.0681
z-bias (mGal)	437.9689	0.5789
x-scale factor (ppm)	67.0709	1.0232
y-scale factor (ppm)	259.3801	1.5024
z-scale factor (ppm)	65.0503	0.6888
θ_{gyz} (arc sec)	-13.1128	0.3978
θ_{gzx} (arc sec)	-0.7195	0.4431
θ_{gzy} (arc sec)	8.6224	0.3346

Table 5: HG1700 accelerometer adjustment results

5.2 Gyroscope Adjustments

The adjustment of the bias-only model given in equation (16) for gyroscopes converged and significant corrections for parameters were done within twenty iterations for both LTN-90-10 and HG1700. This solution and its standard deviations were used as initial information for the adjustment of other models.

All other gyroscope adjustment models didn't work using the proposed method. Although the bias and scale factor model converges, the estimated scale factors and their standard deviations are unrealistic as shown in Table 8. Small errors in biases might have overflowed into scale factors. The bias, scale factor and non-orthogonality model showed unrealistic values for the parameters and their standard deviations. The main reason for these results is mainly due to the earth rotation rate, which is a very weak signal (Britting 1971). This results in that biases and the other parameters can not be separated from. This is somewhat related to the fact that the parameters which can be determined using multi-position

(deg/h)		X	Y	Z
Aug.08	Bias	-0.21	-0.20	0.24
	STD	0.04	0.03	0.03
Aug.09	Bias	-0.23	-0.20	0.24
	STD	0.04	0.03	0.03
Nov.12	Bias	-0.58	-0.24	0.06
	STD	0.04	0.03	0.03
Nov.13	Bias	-0.40	-0.19	0.32
	STD	0.04	0.03	0.03
Dec.14	Bias	-0.20	-0.19	0.24
	STD	0.04	0.03	0.03
Feb.12	Bias	-0.22	-0.20	0.24
	STD	0.04	0.03	0.03

Table 6: LTN-90-100 gyroscope adjustment results for bias-only model (300 iterations)

	X	Y	Z
Bias (deg/h)	3.0875	-1.1981	-0.5969
SD (deg/h)	0.0336	0.0330	0.0557

Table 7: HG1700 gyroscope adjustment result (bias-only model)

static test include only bias and acceleration dependent bias as given in the following observation equations (Titterton and Weston 1997):

$$\omega_{up} = b_{\omega z} - a_{\omega z} g, \quad \omega_{down} = b_{\omega z} + a_{\omega z} g$$

where $b_{\omega z}$ is z-gyroscope bias and $a_{\omega z}$ is acceleration dependent bias.

	Value	STD
x-bias (deg/h)	-0.2022	0.0348
y-bias (deg/h)	-0.2503	0.0257
z-bias (deg/h)	0.2563	0.0332
x-scale factor (ppm)	-497.7	1814.3
y-scale factor (ppm)	-2821.0	1595.6
z-scale factor (ppm)	-462.8	1798.4

Table 8: Result of bias and scale factor model

In summary, the capability of the newly developed method as compared to other calibration methods is listed in Table 9. The advantages of the newly developed calibration method are that it does not require expensive special instruments while calibrating non-orthogonalities as well as scale factors, and the estimated parameters are more accurate than those obtained by standard calibration methods such as the six-position static test.

		LLF	SPS	RT	New
Accel.	Bias	√	√	X	√
	SF	√	√	X	√
	NOTH	√	X	X	√
Gyro.	Bias	√	√	√	√
	SF	X	X	√	X
	NOTH	X	X	√	X
Need Special Instrument		Yes	No	Yes	No

√ : Can be Estimated, X: Cannot be Estimated
SF: Scale Factor, NOTH: Non-orthogonality
LLF: local-level frame, SPS: Six-Position Static
RT: Rate Test, New: the Newly Proposed Method

Table 9: Comparison of calibration methods

6 Conclusions

In this paper, a new calibration method for strapdown INS systems was derived and various calibration models were tested. The main advantage of the newly developed calibration method is that it does not require any expensive calibration faculties. Test results indicate that for accelerometers, biases, scale factors and non-orthogonalities can be determined in a common adjustment using the new method. The time dependent characteristic of accelerometer biases couldn't realistically estimated using the proposed method. On the other hand, using the newly developed method, only the biases can be realistically estimated for gyroscopes. As already indicated by many authors, e.g. Salychev (1998) and Chatfield (1997), the possible reason for this problem is that the earth rotation rate is very a weak signal and small parameters are buried in the noise. Therefore, scale factors and non-orthogonalities must be determined using special instrumentation such as rate tables. If an IMU is mounted on a two-degrees-of-freedom rotational frame where the rotations and the lock during the mission can be accomplished in a programmed manner, low cost systems, which have poor run-to-run stability, can be much benefited by the calibration in the field right before starting the survey mission. A remaining problem, which has not been addressed in this paper, is the determination of the difference between the accelerometer axis system and the gyroscope axis system caused by errors in the installation of the sensors into an IMU.

Acknowledgement

The authors are thankful to Mr. Michael Kern for translating the summary into German.

References

Chatfield, A.B.: Fundamentals of High Accuracy Inertial Navigation. American Institute of Aeronautics and Astronautics (AIAA), Reston, VA, USA, 1997.

Greenspan, R.L.: Inertial Navigation Technology from 1975–1995. NAVIGATION, Journal of the US Institute of Navigation, Vol. 42: 165–186, 1995.

Krakiwsky, E.J.: The Method of Least Squares: A Synthesis of Advances. UCGE Reports No. 10003, Department of Geomatics Engineering, The University of Calgary, Canada, 1990.

Rogers, R.M.: Applied Mathematics in Integrated Navigation Systems, AIAA Education Series, 2000.

Salychev, O.: Inertial Systems in Navigation and Geophysics. Bauman MSTU Press, Moscow, 1998.

Schwarz, K.P. and Wei, M.: INS/GPS Integration for Geodetic Applications. Lecture Notes ENGO623, Department of Geomatics Engineering, The University of Calgary, Canada, 2000.

Schwarz, K.P., and El-Sheimy, N.: Future Positioning and Navigation Technologies. Study performed under the Scientific Services Agreement with Batelle. Columbus Division and Topographic Engineering Center, Fort Belvoir, VA, USA, 1999.

Titterton, D.H. and Weston, J.L.: Strapdown Inertial Navigation Technology. Peter Peregrinus Ltd, London, UK. 1997.

Author's address

Eun-Hwan Shin
MSc. Graduate Student
Department of Geomatics Engineering
The University of Calgary
2500 University Drive N.W.
Calgary, Alberta
Canada, T2N 1N4

Dr. Naser El-Sheimy
Assistant Professor
Department of Geomatics Engineering
The University of Calgary
2500 University Drive N.W.
Calgary, Alberta
Canada, T2N 1N4

Appendix (1)

$$\frac{\partial f_g}{\partial b_{gx}} = -2\left[g_x + g_y \tan\theta_{gyz} + g_z(\tan\theta_{gzx}\tan\theta_{gyz} - \tan\theta_{gzy}/\cos\theta_{gzx})\right]/(1+s_{gx})$$

$$\frac{\partial f_g}{\partial b_{gy}} = -2\left(g_y + g_z \tan\theta_{gzx}\right)/\left(1+s_{gy}\right)\cos\theta_{gyz}$$

$$\frac{\partial f_g}{\partial b_{gz}} = -2g_z/\left(1+s_{gz}\right)\cos\theta_{gzx}\cos\theta_{gzy}$$

$$\frac{\partial f_g}{\partial s_{gx}} = -2\left(l_{gx}-b_{gx}\right)\left[g_x + g_y \tan\theta_{gyz} + g_z(\tan\theta_{gzx}\tan\theta_{gyz} - \tan\theta_{gzy}/\cos\theta_{gzx})\right]/\left(1+s_{gx}\right)^2$$

$$\frac{\partial f_g}{\partial s_{gy}} = \frac{-2(l_{gy}-b_{gy})(g_y + g_z\tan\theta_{gzx})}{(1+s_{gy})^2\cos\theta_{gyz}}$$

$$\frac{\partial f_g}{\partial s_{gz}} = \frac{-2g_z\left(l_{gz}-b_{gz}\right)}{\left(1+s_{gz}\right)^2\cos\theta_{gzx}\cos\theta_{gzy}}$$

$$\frac{\partial f_g}{\partial \theta_{gyz}} = 2\left(g_y + g_z\tan\theta_{gzx}\right)\left[\frac{l_{gx}-b_{gx}}{(1+s_{gx})\cos^2\theta_{gyz}} + \frac{(l_{gy}-b_{gy})\tan\theta_{gyz}}{1+s_{gy}}\right]$$

$$\frac{\partial f_g}{\partial \theta_{gzx}} = 2g_z\left[\left(\tan\theta_{gyz}/\cos^2\theta_{gzx} - \tan\theta_{gzx}\tan\theta_{gzy}\right)\left(\frac{l_{gx}-b_{gx}}{1+s_{gx}}\right) + \frac{1}{\cos^2\theta_{gzx}\cos\theta_{gyz}}\left(\frac{l_{gy}-b_{gy}}{1+s_{gy}}\right) + \frac{\tan\theta_{gzx}}{\cos\theta_{gzy}}\left(\frac{l_{gz}-b_{gz}}{1+s_{gz}}\right)\right]$$

$$\frac{\partial f_g}{\partial \theta_{gzy}} = 2g_z\left[\frac{-1}{\cos\theta_{gzx}\cos^2\theta_{gzy}}\left(\frac{l_{gx}-b_{gx}}{1+s_{gx}}\right) + \frac{\tan\theta_{gzy}}{\cos\theta_{gzx}}\left(\frac{l_{gz}-b_{gz}}{1+s_{gz}}\right)\right]$$

$$\frac{\partial f_g}{\partial l_{gx}} = 2\left[g_x + g_y \tan\theta_{gyz} + g_z(\tan\theta_{gzx}\tan\theta_{gyz} - \tan\theta_{gzy}/\cos\theta_{gzx})\right]/(1+s_{gx})$$

$$\frac{\partial f_g}{\partial l_{gy}} = 2\left(g_y + g_z \tan\theta_{gzx}\right)/\left(1+s_{gy}\right)\cos\theta_{gyz}$$

$$\frac{\partial f_g}{\partial l_{gz}} = 2g_z/\left(1+s_{gz}\right)\cos\theta_{gzx}\cos\theta_{gzy}$$